Facile Preparation of Three-Dimensionally Ordered Macroporous Alumina, Iron Oxide, Chromium Oxide, Manganese Oxide, and Their Mixed-Metal Oxides with High Porosity

Masahiro Sadakane,* Toshitaka Horiuchi, Nobuyasu Kato, Chigusa Takahashi, and Wataru Ueda*

Catalysis Research Center, Hokkaido University, N21, W10, Sapporo, 001-0021, Japan

Received July 11, 2007. Revised Manuscript Received August 23, 2007

This paper describes a facile method to produce three-dimensionally ordered macroporous (3DOM) alumina, iron oxide, manganese oxide, chromium oxide, and their mixed-metal oxides. An ethylene glycol (EG)−methanol mixed solution of metal nitrates was infiltrated into the void of the colloidal crystal template of a monodispersed poly(methyl methacrylate) (PMMA) sphere. Heating initiated nitrate oxidation of the EG to produce metal glyoxylate salt. Further heating converted the glyoxylate salt to metal oxide and decomposed PMMA which produced the desired 3DOM metal oxides. Two important parameters of this method are clarified in order to produce a well-ordered 3DOM structure in high yield: (1) The nitrate oxidation temperature should be lower than the glass transition temperature of the PMMA. (2) The heat produced by oxidative decomposition of the PMMA should effectively be removed. Furthermore, high porosity (66−81%) of the 3DOM materials was confirmed by Hg porosimetry, which can permit facile transport of guest molecules and particles in potential catalysis and filtration.

Introduction

Recently, much attention has been focused on three-dimensionally ordered macroporous (3DOM) materials with pores sized in the submicrometer range because of their application in photonic crystals, catalysis, and separation.[1] To date, the most common synthetic method for the production of 3DOM metal oxides has been an alkoxide-based sol−gel process: (i) a colloidal crystal template is prepared by ordering monodisperse spheres, e.g., polystyrene, poly(methyl methacrylate), or silica, into a face-centered close-packed array (opal structure); (ii) interstices in the colloidal crystal are then filled with liquid metal alkoxides, either neat or in solution, which solidify in situ via a sol−gel transformation, resulting in an intermediate composite structure; (iii) an ordered foam is produced after removing the template by calcination or extraction. The ordered ("inverse opals") structures synthesized by using this method consist of a skeleton surrounding uniform close-packed macropores (Scheme 1, insets). The macropores are interconnected through windows which are formed as a result of the contact between the template spheres prior to infiltration of the precursor solution. Furthermore, the 3DOM materials have high porosity, theoretically ca. 74%. Connected macropores with high porosity can permit facile transport of guest molecules and particles in potential catalysis and filtration.

Scheme 1. Synthesis of 3DOM Metal Oxide Using Ethylene Glycol−Methanol Solution of Metal Nitrate as Precursor Solution and Model of the Inverse Opals Structure (Insets)

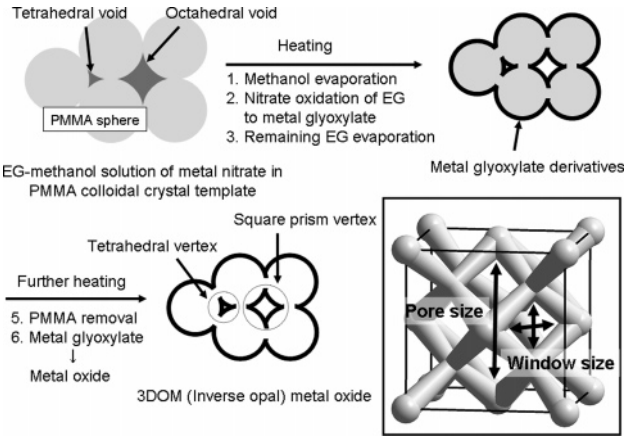

The common alkoxide-based sol−gel method, however, can be applied only to the synthesis of limited metal oxides (generally, Si, Ti, Zr, and mixtures of these) if the metal alkoxide precursor is only moderately reactive.[2] Most of the other metal alkoxides react so quickly that the reaction cannot be controlled. Furthermore, obtaining alkoxide precursors of transition metals and lanthanide metals is difficult and expensive. Commercially available common salts of these metals are usually not suitable for starting materials because of their melting feature. These salts melt at a temperature where the template polymer decomposes and, therefore, do not form the 3DOM structure. Solidification of the transition

* Corresponding authors. Phone: Int.-81-11-706-9166 (M.S.); Int.-81-11-706-9164 (W.U.). Fax: Int.-81-11-706-9163 (M.S.); Int.-81-11-706-9163 (W.U.). E-mail: sadakane@cat.hokudai.ac.jp (M.S.); ueda@cat.hokudai.ac.jp (W.U.).

(1) (a) Schroden, R. C.; Stein, A. In *3D Ordered Macroporous Material, Colloids and Colloid Assemblies*; Caruso, F., Ed.; Wiley-VCH Verlag GmbH and Co. KGaA: Weinheim, Germany, 2004; p 465. (b) Stein, A.; Schroden, R. C. *Curr. Opin. Solid State Mater. Sci.* **2001**, *5*, 553. (c) Stein, A. *Microporous Mesoporous Mater.* **2001**, *44*−*45*, 227.

(2) Holland, B. T.; Blanford, C. F.; Do, T.; Stein, A. *Chem. Mater.* **1999**, *11*, 795.

10.1021/cm071823r CCC: $37.00
Published on Web 10/20/2007

and lanthanide salts before decomposition of the polymer template is necessary.

An alternative method for producing the 3DOM materials of the transition metal oxides was reported by Yan et al.[3] They infiltrated metal salts (acetate or nitrate) into voids in the colloidal crystals and solidified them as oxalate salts by reacting the incorporated metal salts with oxalic acid in the voids. The metal oxalate was converted to metal oxides without melting, which is a key factor in successfully producing 3DOM metal oxides (MgO, Cr_2O_3, Mn_2O_3, Fe_2O_3, Co_3O_4, NiO, and ZnO) materials. In other cases (alumina, SnO_2, or Ln_2O_3), solidification by reacting ammonia[4] or ethylenediaminetetraacetic acid (EDTA)[5] has been reported.

These two-step methods are, however, not suitable for preparation of 3DOM materials of mixed-metal oxides. Each metal has different reactivity with oxalic acid or base, and the produced oxalate salts or metal hydroxides have different solubility in the reacting media, which causes mixed-metal oxides with undesired metal ratio.[6] Synthetic procedures, which ensure chemical homogeneity of the product, are required.

Recently, we have presented a facile one-pot procedure to prepare 3DOM mixed iron oxide, $La_{1-x}Sr_xFeO_{3-\delta}$ ($x = 0-0.4$) and MFe_2O_4 (M = Zn, Ni, or Co), which does not need any alkoxide precursor preparation (Scheme 1).[7] Our strategy was to use an ethylene glycol (EG)−methanol mixed solution of metal nitrate salts, which could be converted to a mixed-metal glyoxylate or metal oxalate derivatives by an in situ nitrate oxidation at low temperature before the template was removed. Further calcination removed the polymer template and converted the glyoxylate salt to mixed-metal oxides, resulting in the well-ordered 3DOM mixed iron oxide materials in high yield.

In this paper, we present the crucial factors of our method, which is applicable to the preparation of 3DOM alumina, iron oxide, chromium oxide, manganese oxide, and their mixed-metal oxides. However, 3DOM materials with other metal (Cu, Ni, Zn, Co, Mg, Ca, La, Ce) oxides could not be obtained. By comparing the thermal analysis of the metal nitrate−EG solutions, we have proposed that the nitrate oxidation temperature should be lower than the glass transition temperature in order to maintain the 3DOM framework under our synthesis condition. Detailed structural characterization of 3DOM alumina, manganese oxide, and iron oxide is described. We have also found that the efficient removal of heat, which was released by oxidative decomposition of PMMA, is important to produce well-ordered 3DOM materials efficiently. For the preparation of 3DOM alumina, decomposition of PMMA is endothermic; therefore, the 3DOM alumina was able to be easily prepared even in a conventional oven. We also demonstrated that the well-ordered 3DOM material prepared with our materials had high (ca. 66−80%) porosity with uniform connecting pore size, which is an attractive feature for potential catalysts and filter materials.

Experimental Section

Materials. All chemicals were reagent grade and used as supplied. All metal nitrates were hydrate forms. Suspensions of monodisperse poly(methyl methacrylate) (PMMA) spheres (diameters, 183 ± 6, 268 ± 9, and 413 ± 15 nm) were synthesized according to standard techniques and packed into colloidal crystals.[7a,8] The obtained template was crushed with an agate mortar, and the obtained particles were adjusted into 0.425−2.000 mm using testing sieves (Tokyo Screen, Co. Ltd.). Quartz sand (10−15 mesh) was purchased from Kokusan Chemical Works (Tokyo).

Characterizations. Powder X-ray diffraction (XRD) patterns were recorded with a diffractometer (Rigaku, RINT Ultima+) using Cu Kα radiation (tube voltage, 40 kV; tube current, 20 mA) equipped with a graphite monochromator. The diffraction line widths were obtained after the subtraction of the instrumental width determined by the line width of silicon powder, and crystallite sizes were calculated from the width of the most intense lines using the Scherrer equation. Cell parameters were calculated using a least-square method from XRD lines (more than six lines). Images of scanning electron microscopy (SEM) were obtained with a JSM-7400F (JEOL) using an accelerating voltage of 1.5 kV. Samples for SEM were dusted on an adhesive conductive carbon paper attached on a brass mount. Images of transmission electron microscopy (TEM) were obtained with a JEM-2000FX (JEOL) using an accelerating voltage of 200 kV with a LaB_6 filament. Samples for TEM were prepared by sonicating small amounts of the powder in 5 mL of ethanol for 1 min and then depositing a few drops of the suspension on a holey carbon grid. Thermogravimetric−differential thermal analysis (TG−DTA) measurements were performed with a TG-8120 (Rigaku) thermogravimetric analyzer. Nitrogen adsorption measurements were performed on an Autosorb 6 (YUASA IONICS) gas adsorption analyzer. Prior to the sorption measurements, the samples were degassed under vacuum at 473 K for 1 h. Surface areas were calculated by the Brunauer−Emmet−Teller (BET) method. Macropores were characterized by a Hg porosimetry experiment using PoreMaster 33P (YUASA IONICS). Pore sizes were calculated using the Washburn equation with a Hg contact angle of 140° and a surface tension of 480 dyn·cm^{-1}. Elemental analyses were performed by the Center for Instrumental Analysis at Hokkaido University. FT-IR spectra were recorded with a Perkin-Elmer Paragon 1000 Fourier transform infrared spectrometer with 2 cm^{-1} resolution.

Synthesis of 3DOM Metal Oxides. Metal nitrate hydrates (metal concentration, 2 M) were dissolved with ca. 5 mL of EG by slow stirring in a 100 mL beaker at room temperature, or 313 K in the case of the aluminum nitrate, until all of the nitrate salt had dissolved, and the produced EG solution was poured into a 25 mL volumetric flask. Methanol (10 mL) and EG were added in amounts necessary to achieve the desired concentration (the final concentration of methanol was 40% by volume). Then, the PMMA colloidal

(3) Yan, H.; Blanford, C. F.; Holland, B. T.; Smyrl, W. H.; Stein, A. *Chem. Mater*. **2000**, *12*, 1134.
(4) (a) Yan, H.; Sokolov, S.; Lytle, J. C.; Stein, A.; Zhang, F.; Smyrl, W. H. *J. Electrochem. Soc*. **2003**, *150*, A1102. (b) Sokolov, S.; Bell, D.; Stein, A. *J. Am. Ceram. Soc*. **2003**, *86*, 1481.
(5) Zhang, Y.; Lei, Z.; Li, J.; Lu, S. *New. J. Chem*. **2001**, *25*, 1118.
(6) (a) Sokolov, S.; Stein, A. *Mater. Lett*. **2003**, *57*, 3593. (b) Yan, H.; Blanford, C. F.; Lytle, J. C.; Carter, C. B.; Smyrl, W. H.; Stein, A. *Chem. Mater*. **2001**, *13*, 4314. (c) Yan, H.; Blanford, C. F.; Smyrl, W. H.; Stein, A. *Chem. Commun*. **2000**, 1477.
(7) (a) Sadakane, M.; Takahashi, C.; Kato, N.; Ogihara, H.; Nodasaka, Y.; Doi, Y.; Hinatsu, Y.; Ueda, W. *Bull. Chem. Soc. Jpn*. **2007**, *80*, 677. (b) Sadakane, M.; Takahashi, C.; Kato, N.; Asanuma, T.; Ogihara, H.; Ueda, W. *Chem. Lett*. **2006**, *35*, 480. (c) Sadakane, M.; Asanuma, T.; Kubo, J.; Ueda, W. *Chem. Mater*. **2005**, *17*, 3546.
(8) (a) Zou, D.; Ma, S.; Guan, R.; Park, M.; Sun, L.; Aklonis, J. J.; Salovey, R. *J. Polym. Sci., Part A: Polym. Chem*. **1992**, *30*, 137. (b) Lytle, J. C.; Yan, H.; Ergang, N. S.; Smyrl, W. H.; Stein, A. *J. Mater. Chem*. **2004**, *14*, 1616.

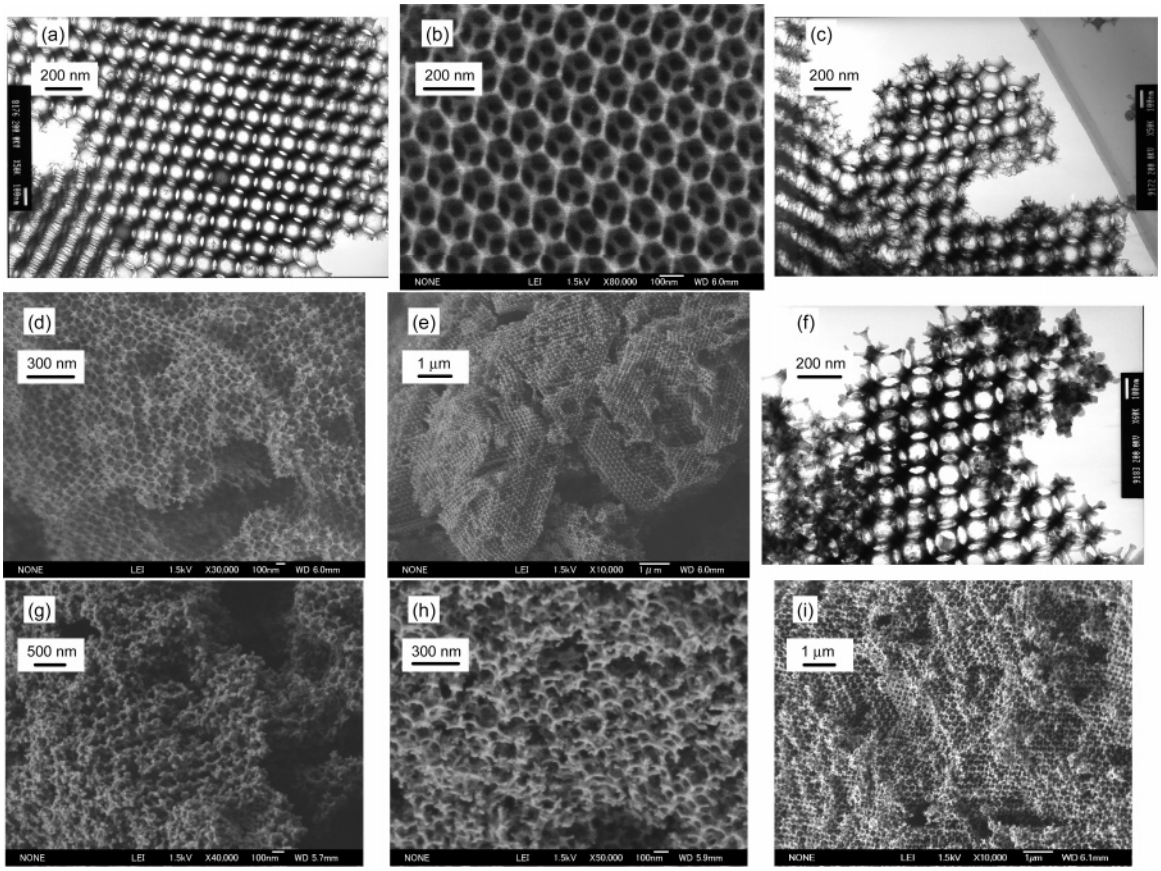

Figure 1. TEM and SEM images of solid materials obtained after calcination at 673 K of PMMA (diameter, 291 nm) colloidal crystal infiltrated by EG−methanol (40 vol %) mixed solution of $M(NO_3)_x$ (metal concentration, 2 M) M = Al ($x = 3$) (a and b), Fe ($x = 3$) (c−e), Mn ($x = 2$) (f and g), and Cr ($x = 3$) (h and i) (iPMMA (diameter, 416 nm) was used). Calcination rate was 1 K·min^{-1}, and the calcination temperature was maintained for 5 h.

Table 1. Metal Dependence on the Formation of 3DOM Material

metal	Fe	Cr	Al	Cu	Mn	Ce	Co	Zn	Ni	La	Mg	Ca
3DOM[a]	A	B	A	D	C	D	D	D	D	D	D	D
crystal phase	Fe_2O_3	Cr_2O_3	amor	CuO	Mn_2O_3, Mn_3O_4	CeO_2	Co_3O_4	ZnO	NiO	$La_5O_7NO_3$ $La_2O_2CO_3$	MgO	$CaCO_3$
crystallite size [nm][b]	19	39		18		8	17	9	12		7	42
ox. temp [K][c]	328	335	342	375	377	383	386	388	392	403	413	N.O.[d]

[a] A: well-ordered 3DOM structure was observed by SEM, and the fraction of 3DOM was more than 95% (more than 20 particles were randomly chosen by SEM, and the images with magnifications of 5000−10000× were taken. The fraction of 3DOM was calculated as follows: number of particles which contain the 3DOM structure/total number of particles). B: more than 95% of the samples contained 3DOM structure, but not well-ordered. C: ca. 60% of samples contained well-ordered 3DOM structure. D: only a very small part of the sample has 3DOM structure (fraction of 3DOM was less than 5%), or porous structure was hardly observed by SEM. [b] Crystallite sizes were calculated from the width of the most intense line using the Scherrer equation corrected for instrumental broadening. [c] Obtained from TG−DTA. [d] Not observed.

crystals were soaked in the solution for 3 h. Excess solution was removed from the impregnated PMMA colloidal crystals by vacuum filtration. The obtained sample was allowed to dry in air at room temperature overnight. A 0.5 g amount of the sample was mixed with 2.5 g of quartz sand (10−15 mesh) and calcined in a tubular furnace (i.d. ca. 22 mm) in an air flow (50 mL·min^{-1}). The temperature was raised at a rate of 1 K·min^{-1} to 673 K and held for 5 h. After the calcination, the obtained powder sample was separated from the mixed quartz sand using testing sieves, where bigger quartz sand remained on the testing sieves.

Results and Discussion

Scope of Metal. In order to clarify the scope of metals for 3DOM materials using our EG in situ nitrate oxidation method, we tested nitrate salts of Ni, Co, Mn, Cu, Fe, Cr, Zn, Mg, Ca, Al, La, and Ce as a starting metal source. After calcination at 673 K, the obtained samples were checked by SEM and TEM. As shown in Figure 1a−e, well-ordered 3DOM structures of alumina and iron oxide were obtained in high yield. Large fractions (more than 95% of particles by SEM images) of the sample had highly ordered porous structure in three dimensions over a range of tens of micrometers. In the case of manganese oxide, 3DOM structure was observed (Figure 1f) but contained agglomerates of nanosized particles (Figure 1, parts f and g). In the case of chromium oxide, 3DOM structure of Cr_2O_3 was not well-ordered compared to others (Figure 1h) due to crystal growth of the Cr_2O_3 (39 nm, Table 1). It is known that growth of crystallite size destroys the 3DOM structure.[4b,7] Also, in the case of iron oxide and manganese oxide as described below, 3DOM structure collapses when the crys-

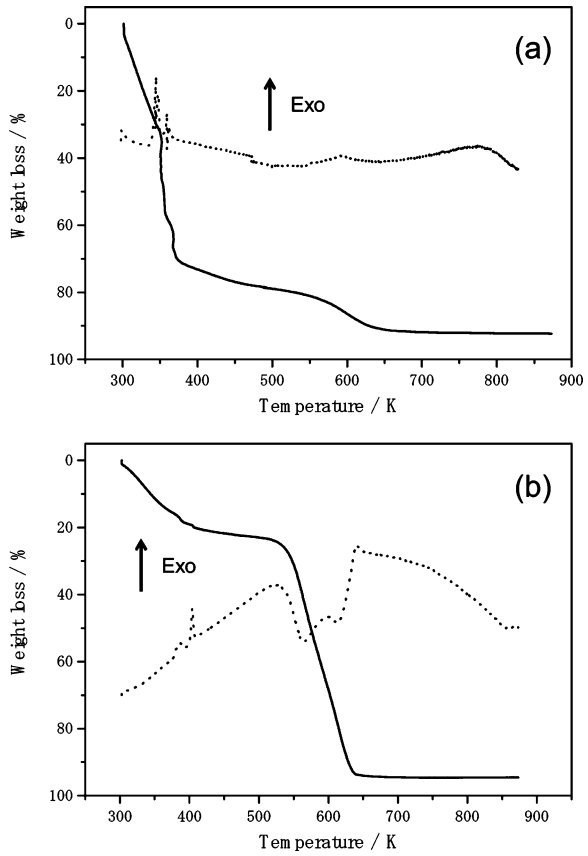

Figure 2. TG−DTA curves of EG−methanol solution of $Al(NO_3)_3 \cdot 9H_2O$ (2 M) (a) and PMMA filled with the EG−methanol solution of $Al(NO_3)_3 \cdot 9H_2O$ (2 M) (b) at a heating rate of 1 K·min^{-1}. Air flow rate was 30 mL·min^{-1}.

tallite size exceeds ca. 40 nm. By increasing the PMMA sphere to 413 nm, 3DOM structure of Cr_2O_3 was able to be obtained (Figure 1i). On the other hand, in the case of other metals, very small fractions of the samples had 3DOM structure (less than 5% of particles observed by SEM had 3DOM structure). We have succeeded in producing 3DOM structure of iron oxides mixed with Zn, Ni, Co, or La;[7] however, 3DOM structure could not be obtained with these metals alone.

In order to understand the metal dependency, the calcination process was analyzed by TG−DTA. The TG−DTA curve of a EG−methanol solution containing $Al(NO_3)_3 \cdot 6H_2O$ without the PMMA template is shown in Figure 2a. Weight loss from room temperature to ca. 340 K with an endothermic DTA peak corresponds to methanol and H_2O evaporation. Weight loss from 342 to 360 K with an exothermic peak was observed. This weight loss corresponds to the reaction of EG with metal nitrate to produce metal glyoxylate ($[C_2H_2O_4]^{2-}$) or oxalate ($[C_2O_4]^{2-}$) and NO_x gas. The IR spectrum of a solid obtained after calcination of the EG−methanol solution containing $Al(NO_3)_3 \cdot 6H_2O$ at 523 K has carbonyl peaks (1722, 1699, and 1639 cm^{-1}), which are similar to carbonyl peaks (1723 and 1695 cm^{-1}) of commercial $Al_2(C_2O_4)_3 \cdot nH_2O$ (Supporting Information Figure S1). Stefanescu and co-workers have reported a similar reaction in aqueous media,[9] which was similar to the reaction we found in our synthesis of 3DOM $LaFeO_3$ and $ZnFe_2O_4$.[7a,b] The weight loss up to 473 K was ca. 78%, indicating the presence of the desired Al−glyoxylate.[10] We also heated the solution in an oil bath and observed brown gas evolution (the color of NO_x) at around 373 K. The weight decrease continued up to ca. 773 K with a total weight loss of 92%, indicating the presence of Al_2O_3.[10]

The nitrate oxidation temperatures, estimated by using TG−DTA (starting temperature of weight decrease), produced crystal phases, and crystallite sizes, based on XRD patterns, are summarized in Table 1. It is known that the metal salts should be solidified before the PMMA is removed, and Yan et al. succeeded in producing 3DOM MgO, Cr_2O_3, Mn_2O_3, Fe_2O_3, Co_3O_4, NiO, and ZnO by converting metal nitrate or metal acetate to metal oxalate salts before the PMMA decomposition.[3] In our methods, all metal nitrates except for $Ca(NO_3)_2$ were converted to the metal oxalate derivatives at a temperature where PMMA decomposes (ca. 510−630 K). However, only 3DOM materials of iron oxide, alumina, manganese oxide, and chromium oxide were able to be obtained. Nitrate oxidation temperatures of these metal nitrates were relatively low (328−377 K) compared to the others, indicating that other heating-related events should be considered. The glass transition temperature of PMMA is important for the 3DOM preparation in our method, that of our PMMA is ca. 380 K, because above this temperature PMMA melts and the void space between the PMMA spheres decreases.[7a,11] Therefore, the nitrate oxidation should be completed before the PMMA starts to melt. In our previous paper,[7c] we have indicated that the presence of methanol increased the 3DOM structure yield. By melting of the PMMA, the solution in the void is squeezed out. Methanol evaporated before the melting of the PMMA, made space in the void, and reduced the amount of the solution which was squeezed out from the voids. In the case of Fe, Al, and Cr where well-ordered 3DOM structure was obtained in high yield, the nitrate oxidation was lower than the PMMA glass transition temperature and these solidified sufficiently in the void. On the other hand, in the case of Mn and Cu, the nitrate oxidation temperature was comparable to the PMMA glass transition temperature. Solidification by nitrate oxidation and melting of the PMMA occurred at the same time, and some of the metal salts were squeezed out from the void in the template causing low fraction of 3DOM structure.

Structural Characterization of Iron Oxide, Manganese Oxide, and Alumina. As summarized in Tables 2−4, alumina, iron oxide, and manganese oxide were carefully investigated by increasing the calcination temperature and their crystal phase, crystallite size, BET surface area, pore size, window size, and remaining organic element.

In the case of alumina, 3DOM structure was maintained until the calcination temperature reached 1473 K. The crystal system of the obtained material was amorphous until the

(9) (a) Caizer, C.; Stefanescu, M. *J. Phys. D: Appl. Phys.* **2002**, *35*, 3035. (b) Stefanescu, M.; Sasca, V.; Birzescu, M. *J. Therm. Anal. Calorim.* **1999**, *56*, 579.
(10) The density of the EG−methanol solution containing $Al(NO_3)_3$ (2 M) was 1.24 g·cm^{-3}. The production of $Al_2(C_2H_2O_4)_3$ and Al_2O_3 corresponds to weight loss of 74% and 92%, respectively.
(11) Sen, T.; Tiddy, G. J. T.; Casci, J. L.; Anderson, N. W. *Chem. Mater.* **2004**, *16*, 2044.

Table 2. Structural Data for Samples of Al_2O_3 Prepared at Different Calcination Temperatures

calcd temp [K]	3DOM[a]	crystal phase	BET surface area [$m^2 \cdot g^{-1}$]	crystallite size [nm][b]	pore size [nm][c]	window size [nm][c]	elemental analysis [wt %] C	N	H	S
673	A	amor	74		148 ± 2	$57 \pm 3 \times 55 \pm 3$	2.2	0	1.4	0.35
773	A	amor	75				1.1	0	1.2	0.4
873	A	amor	60		136 ± 3	$58 \pm 5 \times 51 \pm 5$	1.45	0	1.0	0.4
973	A	amor	72				1.9	0	1.0	0.45
1073	A	amor	60		147 ± 2	$59 \pm 5 \times 59 \pm 3$	0.7	0	1.0	0.3
1173	A	γ-Al_2O_3	70				0	0	0.8	0
1273	A	γ-Al_2O_3	57		160 ± 4	$76 \pm 4 \times 65 \pm 5$	0	0	0.6	0
1373	A	γ-Al_2O_3 + δ-Al_2O_3	35				0	0	0.5	0
1473	A	δ-Al_2O_3 + α-Al_2O_3	21		137 ± 3	$56 \pm 4 \times 47 \pm 3$	0	0	0.5	0
1573	D	α-Al_2O_3	<1	67			0	0	0.3	0
1673	D	α-Al_2O_3	<1	87			0	0	0.4	0

[a] A: well-ordered 3DOM structure was observed by SEM, and the fraction of 3DOM was more than 95% (more than 20 particles were randomly chosen by SEM, and the images with magnifications of 5000−10000× were taken. The fraction of 3DOM was calculated as follows: number of particles which contain the 3DOM structure/total number of particles). D: 3DOM structure was not observed by SEM. [b] Crystallite sizes were calculated from the width of the (113) line (JCPDS: 46-1212) using the Scherrer equation corrected for instrumental broadening. [c] Pore sizes corresponding to the distance between the centers of two neighboring open spheres and window sizes were averaged over 20 sizes estimated by the (110) direction of the TEM images.

Table 3. Structural Data for Samples of Mn_2O_3 Prepared at Different Calcination Temperatures

calcd temp [K]	3DOM[a]	crystal phase	BET surface area [$m^2 \cdot g^{-1}$]	crystallite size [nm][b]	pore size [nm][c]	window size [nm][c]	elemental analysis [wt %] C	N	H	S
673	C	Mn_2O_3 + Mn_3O_4	53		176 ± 2	$87 \pm 6 \times 85 \pm 7$	0	0	0	0.5
773	C	Mn_2O_3	32	36			0	0	0	0.5
873	D	Mn_2O_3	20	41			0	0	1.0	0.4
973	D	Mn_2O_3	19	46			0	0	0.4	0

[a] C: ca. 60% of samples contained well-ordered 3DOM structure. D: 3DOM structure was not observed by SEM. [b] Crystallite sizes were calculated from the width of the (222) line (JCPDS: 24-0508) using the Scherrer equation corrected for instrumental broadening. [c] Pore sizes corresponding to the distance between the centers of two neighboring open spheres and window sizes were averaged over 20 sizes estimated by the (110) direction of the TEM images.

Table 4. Structural Data for Samples of Fe_2O_3 Prepared at Different Calcination Temperatures

calcd temp [K]	3DOM[a]	crystal phase	BET surface area [$m^2 \cdot g^{-1}$]	crystallite size [nm][b]	pore size [nm][c]	window size [nm][c]	elemental analysis [wt %] C	N	H	S
673	A	Fe_2O_3	57	19	170 ± 10	$82 \pm 16 \times 74 \pm 13$	0	0	0.3	0.3
773	A	Fe_2O_3	35	36			0	0	0.3	0.3
873	D	Fe_2O_3	26	41			0	0	0	0.35
973	D	Fe_2O_3	13	54			0	0	0	0

[a] A: well-ordered 3DOM structure was observed by SEM, and the fraction of 3DOM was more than 95% (more than 20 particles were randomly chosen by SEM, and the images with magnifications of 5000−10000× were taken. The fraction of 3DOM was calculated as follows: number of particles which contain the 3DOM structure/total number of particles). D: 3DOM structure was not observed by SEM. [b] Crystallite sizes were calculated from the width of the (104) line (JCPSD: 33-0664) using the Scherrer equation corrected for instrumental broadening. [c] Pore sizes corresponding to the distance between the centers of two neighboring open spheres and window sizes were averaged over 20 sizes estimated by the (110) direction of the TEM images.

calcination temperature reached 973 K, γ-Al_2O_3 between 1073 and 1273 K, γ- and δ-Al_2O_3 at 1373 K, δ- and α-Al_2O_3 at 1473 K, and α-Al_2O_3 more than 1573 K. The BET surface area started to decrease when the amorphous Al_2O_3 started to crystallize and was <1 $m^2 \cdot g^{-1}$ when the big crystal of α-Al_2O_3 grew and, therefore, the 3DOM structure collapsed. The pore size and window size estimated by using TEM image (Figure 3) were ca. 150 and 57 nm, respectively, and did not change in response to increasing temperature. The pore size was ca. 52% of the original PMMA sphere because of melting of the PMMA sphere.[6c,11] Carbon and sulfur remained up to 1073 K, whereas no nitrogen was observed at 673 K. The structure of the 3DOM is a so-called "shell structure" in case of amorphous alumina, where the surface of the template sphere is covered by the alumina. Crystallization changes the "shell structure"[12] to a "skeleton structure", where tetragonal vertices and square prism vertices are connected by strutlike bonds, as reported in the case of our 3DOM ferrite[7a] and others.[4b,13,14]

In the case of iron oxide and manganese oxide, the 3DOM structure was maintained up to 773 K. In comparison to mixed iron oxide such as $LaFeO_3$ and $ZnFe_2O_4$, iron oxide crystal grows faster and destroys the 3DOM structure. In iron oxide and manganese oxide, carbon and sulfur can be more easily removed from the materials than alumina due to the high oxidative activity of iron and manganese. Pore

(12) (a) Wijnhoven, J. E. G. J.; Vos, W. L. *Science*, **1998**, *281*, 538. (b) Richel, A.; Johnson, A. N. P.; McComb, D. W. *Appl. Phys. Lett*. **2000**, *76*, 1816. (c) Wijnhoven, J. E. G. J.; Bechger, L.; Vos, W. L. *Chem. Mater*. **2001**, *13*, 4486. (d) Wang, D.; Caruso, F. *Adv. Mater*. **2003**, *15*, 205.
(13) Blanford, C. F.; Yan, H.; Schroden, R. C.; Al-Daous, M.; Stein, A. *Adv. Mater*. **2001**, *13*, 401.
(14) (a) Dong, W.; Bongard, H. J.; Tesche, B.; Marlow, F. *Adv. Mater*. **2002**, *14*, 1457. (b) Dong, W.; Bongard, H. J.; Marlow, F. *Chem. Mater*. **2003**, *15*, 568.

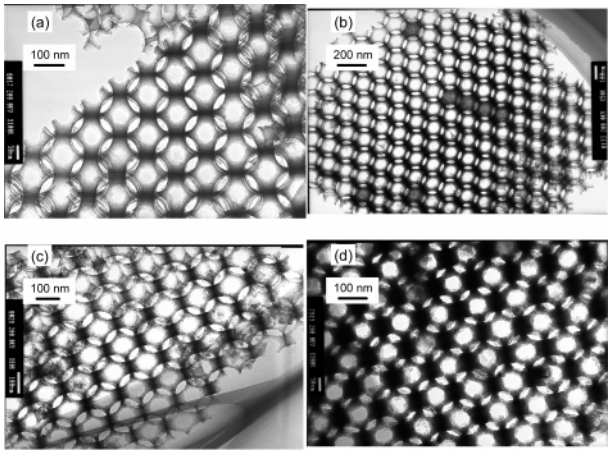

Figure 3. TEM images of 3DOM alumina materials. Calcination temperature: 873 (a), 1073 (b), 1273 (c), and 1473 K (d).

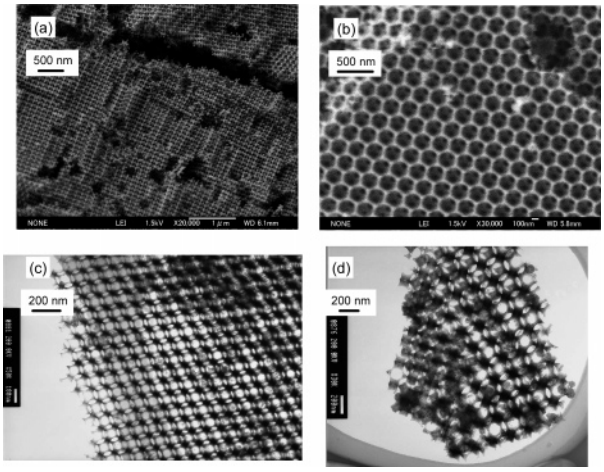

Figure 4. SEM and TEM images of 3DOM alumina. The diameters of PMMA are 183 (a and c) and 413 nm (b and d).

size and window size were ca. 170 and 80 nm for both iron oxide and manganese oxide, which correspond to ca. 42% shrinkage from the original PMMA sphere.

Easy Preparation of 3DOM Alumina. Decomposition of PMMA with and without Fe ion is always an exothermal reaction, and the removing of this heat is important to produce 3DOM structure. Therefore, we have always diluted our infiltrated PMMA template with quartz sand.[7] Furthermore, a low heating rate (1 $K \cdot min^{-1}$) and air flow (50 $mL \cdot min^{-1}$) for 0.5 g of the infiltrated PMMA template mixed with 2.5 g of quartz in a ca. 22 mm tube is crucial to produce 3DOM materials. Removing quartz sand is a time-consuming step and scale-up is difficult.

We have found that decomposition of PMMA in the case of alumina is endothermic under our conditions. Figure 2b shows the TG−DTA chart of the EG−methanol solution containing $Al(NO_3)_3$ (2 M) infiltrated in a PMMA template. The weight loss up to ca. 500 K corresponded to the evaporation of the methanol, the NO_x, and the remaining EG. The big weight loss between 500 and 600 K with an endothermal peak corresponded to the degradation of the PMMA and $Al_2(C_2H_2O_4)_3$ to produce the alumina.

Once we can produce well-ordered 3DOM alumina without quartz sand and air flow in a conventional oven, future scale-up is promising. Furthermore, we can control pore sizes by changing the size of PMMA (Figure 4). The pore sizes and window sizes related to that of PMMA are summarized in Table 5.

Table 5. Pore Sizes and Window Sizes Estimated by TEM and Hg Porosimetry

PMMA [nm]	crystal phase[a]	pore size [nm][b]	window size [nm][b]	pore size [nm]	porosity [%]
183	γ-Al_2O_3	116 ± 4	$54 \pm 6 \times 49 \pm 4$	50	
268	γ-Al_2O_3	160 ± 4	$76 \pm 4 \times 65 \pm 5$	67	81
413	γ-Al_2O_3	243 ± 7	$105 \pm 7 \times 98 \pm 7$	88	66

[a] Sample was made by calcination temperature of 1273 K. [b] Pore sizes corresponding to the distance between the centers of two neighboring open spheres and window sizes were averaged over 20 sizes estimated by the (110) direction of TEM images.

Table 6. Lattice Constants of 3DOM Mixed-Metal Oxides

sample	calcd temp [K]	crystal system[a]	lattice constant [Å][a],*b*	crystallite size [nm][c]
$ZnAl_2O_4$	873	cubic	$a = 8.1128 \pm 24$ (8.0848)	31
$LaAlO_3$	1073	hexagonal	$a = 5.3657 \pm 9$ (5.3640)	37
			$c = 13.0955 \pm 57$ (13.1100)	
$LaCrO_4$	773	monoclinic	$a = 7.0316 \pm 24$ (7.0369)	56
			$b = 7.2276 \pm 32$ (7.2348)	
			$c = 6.6927 \pm 27$ (6.6918)	
			$\beta = 104.96 \pm 4$ (104.95) deg	
$ZnCr_2O_4$	873	cubic	$a = 8.3270 \pm 29$ (8.3275)	13
$LaMnO_3$	973	hexagonal	$a = 5.5167 \pm 60$ (5.5230)	28
			$c = 13.3573 \pm 230$ (13.3240)	

[a] Lattice constants were calculated from XRD data. [b] Values in parentheses were reported value in the JCPDS data 05-0669, 31-0022, 22-1107, and 32-0484 for ZnAl2O_4, $LaAlO_3$, $ZnCr_2O_4$, and $LaMnO_3$, respectively, and ref 15 for $LaCrO_4$. [c] Crystallite sizes of $ZnAl_2O_4$, $LaAlO_3$, $LaCrO_3$, $ZnCr_2O_4$, and $LaMnO_3$ were calculated from the width of the (311), (110), (200), (311), and (102) line using the Scherrer equation corrected for instrumental broadening.

Preparation of 3DOM Mixed-Metal Oxides. We have reported that 3DOM materials of several mixed iron oxides can be obtained by using our method.[7] 3DOM mixed aluminum, manganese, and chromium oxides can be prepared. SEM images are presented in Supporting Information Figures S2−S6, and the crystal systems, lattice parameters, and crystallite sizes are summarized in Table 6. 3DOM mixed-metal oxides ($ZnAl_2O_4$, $LaAlO_3$, $LaCrO_4$, $ZnCr_2O_4$, and $LaMnO_3$) materials were obtained with the desired crystal system. In the case of $LaCrO_4$,[15] it was difficult to maintain the 3DOM structure because of rapid crystal growth. After calcinations at 773 K, the 3DOM structure started to collapse (Supporting Information Figure S5a) and the crystallite size was ca. 56 nm. By decreasing the calcination temperature to 723 K, well-ordered 3DOM structure was obtained (Supporting Information Figure S5, parts b and c), but the obtained material was amorphous. Once the $LaCrO_4$ was formed the crystallite grew faster than the other metal oxides and started to destroy the 3DOM structure. More careful calcination or increasing of the PMMA sphere diameter (as described for the synthesis of Cr_2O_3) is necessary to produce well-ordered 3DOM $LaCrO_4$. These materials can be good candidates for catalysts, SOFC electrodes, optical and magnetic materials, and the introduction of well-ordered porosity is expected to control the performance. In addition to our previous reports,[7] our method is a versatile and facile one for the production of 3DOM mixed-metal oxides of aluminum, iron, manganese, and chromium, which overcomes the previously reported faults regarding difficulty in

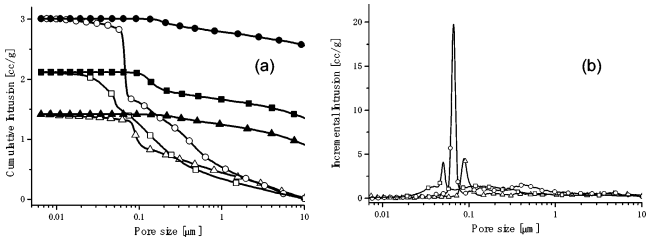

Figure 5. Hg porosimetry results of 3DOM alumina. The diameters of PMMA are 183 (squares), 268 (circles), and 413 nm (triangles). Open symbols represent intrusion and closed ones represent extrusion.

keeping the desired metal ratio[6] or requirement for repeating presynthesis of alkoxide precursors.[16]

Porosity. Porosity was measured using Hg porosimetry. The cumulative and incremental intrusion was plotted against pore diameter for three 3DOM alumina samples prepared with PMMA spheres of 183, 268, and 413 nm (Figure 5). The Hg intrusion in the low-pressure region (ca. 0.1−10 μm) was due to interparticle voids and cracks in the particles, which were observed on the surface of particles (for example, Figure 1, parts d and e, Figure 4, parts a and b). The sharp increase of the Hg intrusion was due to the interconnecting windows between the macropores. From the peak top of the incremental intrusion spectra (Figure 5b) the window size was estimated that is similar to the short window sizes estimated by TEM, summarized in Table 5. The increase of Hg intrusion due to the window of the sample prepared using the smallest PMMA sphere (183 nm) was not clear, and pores smaller than the window size were detected. This is due to the pores not being as well-ordered as those of the other two samples. In our ferrite case, 3DOM fraction of the sample made by the smaller PMMA spheres was less than that of samples made by the bigger spheres.[7a]

Porosity was calculated from the amount of intrusion Hg in the pores.[17] The porosity of samples made by PMMA with 268 and 413 nm was 81% and 66%, respectively. These values were close to the theoretical value (74%) for the porosity of inverse opals, indicating that samples made by our method have the desired 3DOM structure quantitatively.

Conclusion

Together with our previous paper,[7] we have demonstrated that 3DOM materials of alumina, iron oxide, manganese oxide, chromium oxide, and their mixed-metal oxides could be prepared using our facile one-pot procedure in high yields. The most important factor to produce the desired 3DOM structure is that the nitrate oxidation temperature should be lower than the glass transition temperature of PMMA. High porosity of the 3DOM materials, which is an attractive feature for application as future catalysts and filters, was able to be confirmed by using Hg porosimetry. Furthermore, we demonstrated that the removal of heat produced by oxidative decomposition of PMMA is important to keep the 3DOM structure. In the case of alumina, PMMA decomposition is an endothermic process (not oxidative decomposition) and the heat release treatment such as mixing with diluent or gas flow is not necessary. Therefore, 3DOM alumina can be produced even in a conventional oven without any diluent and gas flow, which is attractive for future scale-up.

Acknowledgment. We thank Mr. Kenji Sugawara (High Voltage Electron Microscope Laboratory, Center for Advanced Research of Energy Conversion Materials, Hokkaido University) and Mr. Yoshinobu Nodasaka (Laboratory of Electron Microscopy, Graduate School of Dental Medicine, Hokkaido University) for running TEM measurements. We thank Grants-in-Aid for Scientific Research (Scientific Research "B", No. 18360383) for financial support. We thank YUASA IONICS (Osaka) for performing mercury porosimetry.

Supporting Information Available: IR of ethylene glycol, solid obtained after calcination of EG−methanol solution containing $Al(NO_3)_2 \cdot 6H_2O$ at 473 K in air, and $Al_2(C_2O_4)_3 \cdot nH_2O$ (Wako Chemical) (Figure S1), SEM images of 3DOM $ZnAl_2O_4$ (Figure S2), SEM images of 3DOM $LaAlO_3$ (Figure S3), SEM image of 3DOM $LaMnO_3$ (Figure S4), SEM images of 3DOM $LaCrO_4$ (Figure S5), and SEM images of $ZnCr_2O_4$ prepared at 873 K (Figure S6) (PDF). This material is available free of charge via the Internet at http://pubs.acs.org.

CM071823R

(15) Aoki, Y.; Konno, H.; Tachikawa, H.; Inagaki, M. *Bull. Chem. Soc. Jpn.* **2000**, *73*, 1197.
(16) (a) Kim, Y. N.; Kim, S. J.; Lee, E. K.; Chi, E. O.; Hur, N. H.; Hong, C. S. *J. Mater. Chem.* **2004**, *14*, 1774. (b) Chi, E. C.; Kim, Y. N.; Kim, J. C.; Hur, N. H. *Chem. Mater.* **2003**, *15*, 1929. (c) Kim, Y. N.; Chi, E. O.; Kim, J. C.; Lee, E. K.; Hur, N. H. *Solid State Commun.* **2003**, *128*, 3546.
(17) Porosity was calculated using a density of alumina of 0.303 $mL \cdot g^{-1}$.